

## CFD Simulation Study of The Novel Multistage Inlet Gasifier for Enhancement of Syngas Production

Muhammad Irfan Rosli<sup>1</sup>, Nor Afzanizam Samiran<sup>1\*</sup>

<sup>1</sup>Department of Mechanical Engineering Technology, Faculty of Engineering Technology,  
Universiti Tun Hussein Onn Malaysia, 86400 Pagoh, Johor, MALAYSIA

\*Corresponding Author Designation

DOI: <https://doi.org/10.30880/peat.2022.03.02.071>

Received 07 November 2022; Accepted 07 November 2022; Available online 10 December 2022

**Abstract:** Economically, fossil fuels remain the main source of energy despite their high emissions of greenhouse gases. However, biomass, a renewable fuel with CO<sub>2</sub> neutrality, has experienced widespread attention as a potential contributor to the sustainable development of the energy sector. Gasification is an important thermochemical process that converts biomass feedstock into H<sub>2</sub>-rich combustible gases known as syngas. Its main product (syngas) can be used as fuel in various conversion technologies to produce different products, including electricity and chemicals. This research study focuses particularly on biomass gasification that is a promising technology to achieve high-quality syngas in the presence of one or more gasification agents. To accomplish this aim, a single-stage and two-stage downdraft reactor are analysed in this study using an equilibrium model with non-premixed combustion in the ANSYS Fluent. This study shows that the CFD model simulated values of outlet gas composition was in good agreement and was validated with the Paul<sup>1</sup> model prediction and experimental data<sup>2</sup>. The highest temperature inside the gasifier for a single stage model is found in the oxidation zone, where the air is supplied. The temperature in the drying zone is less than 460 K, in the pyrolysis zone is between 470 and 455 K, in the oxidation zone is between 470 and 490 K, and in the reduction zone is between 480 and 485 K. The highest temperature inside the gasifier for a double stage model is found in the oxidation zone, where the air is supplied. The temperature in the drying zone is less than 470 K, in the pyrolysis zone is between 470 and 480 K, in the oxidation zone is between 470 and 520 K, and in the reduction zone is between 480 and 485 K. It is observed that the CO and H<sub>2</sub> concentrations are higher in the pyrolysis zone for single and double stage as the volatile matter turn to gases phase due devolatilization process. Then for CH<sub>4</sub> mole fraction, the single stage was 0.06 % while the double stage was 0.03 %.<sup>3</sup> reported CH<sub>4</sub> values similar to those found in this study. It is demonstrated the advantages of the double stage by supply air in gasification experiments in a downdraft gasifier.

**Keywords:** Gasification, Gasification Agents, Computational Fluid Dynamic (CFD)

## 1. Introduction

Energy demand has risen in recent years, and this will almost certainly increase fossil fuel consumption, resulting in an increase in CO<sub>2</sub> emissions<sup>4</sup>. According to the International Energy Agency, Southeast Asia is a remarkable group of countries with variations in the scale and patterns of energy consumption<sup>5</sup>. It is shown that energy demand in Southeast Asia has increased by more than 80% between 2015 and 2035; this increase is comparable to Japan's current demand<sup>6</sup>. According to the report, fossil-fuel subsidies in Southeast Asia worth Usd51 billion in 2012<sup>6</sup>. It has been discovered that over 130 million people in Southeast Asia still lack access to electricity. Renewable energy deployment can help secure energy supplies while also mitigating climate change issues by reducing fossil fuel consumption, which benefits the environment and is sustainable<sup>7</sup>. Syngas is known as one of the potential clean renewable energy in power generation sector which typically produced via gasification technology.

Syngas produced from the gasification process consists of a mixture of H<sub>2</sub>, carbon monoxide (CO), carbon dioxide (CO<sub>2</sub>), and methane (CH<sub>4</sub>), depending on the fuel composition and gasifying agent<sup>8</sup>. Syngas could generate electrical power and heat in an engine/gas turbine, steam turbine, fuel cells and produce value-added chemicals like methanol, urea, ammonia, and diesel fuel<sup>9</sup>. Steam gasification is a good process that results in higher product yield and H<sub>2</sub> concentration, which are important parameters for evaluating syngas quality and system performance<sup>10</sup>. It can also provide a higher heating value when compared to gasification in oxygen and air atmosphere<sup>10</sup>. The composition of syngas is determined by some factors, including the type of biomass used in the process, the temperature, and the type of gasification agent used<sup>11</sup>. The present study focused on the effect of gasifying agent.

Gasification is an environmentally friendly and efficient way of managing carbon-based materials in the presence of steam, air, and pure oxygen for the production of hydrogen (H<sub>2</sub>)<sup>12</sup>. A study of biomass gasification discovered that gasification under steam atmosphere has a higher exergy efficiency than gasification under air atmosphere. Gasifying agent and fuel are not the only parameters that can influence gasification performance; gasifier type, the particle size of feedstock, and operational conditions can also impact<sup>10</sup>.

The majority of downdraft gasifier modelling studies are based on reactors with a single stage of gasification fluid supply using air. There are few studies in the literature that study the effects of a double-stage on gasification products and other parameters<sup>13</sup>. The biomass gasification process in a two-stage downdraft reactor is analyzed in this work using an equilibrium model with non-premixed combustion. This approach because the biomass and oxidizer enter the reaction zone in separate streams. Because of its low rate of tar yield, a two-stage downdraft gasifier was selected because it is more suitable for low- and medium-scale power generation applications<sup>14</sup>.

## 2. Methodology

This study begins with collecting information through the analysis of numerous journals and articles on the subject of gasification by different means of gasification. The analysis of the problem statement, the objective of study and scope, and the importance of analysis in this present work need to be reviewed based on the previous research. This study then continues with the development of the Solidworks single-stage downdraft gasifier and model specifications apply to the design based on the collection of data from the review of previous studies. Then the models are imported for the simulation process into the ANSYS Design Suite. Next, the model have to generate meshing in ANSYS Design Suite. The simulation study begins with the setup of the model compartment parameters and boundary conditions. In this case, when the simulation runs out, the model needs to be redesigned. Meantime, data will be interpret the outline the temperature distribution and syngas composition based on the simulation. Finally, the conclusion of this study will be discussed.

## 2.1 Material section

The ultimate and proximate analytical data from rubber wood are used for validation, as shown in Table 1.

**Table 1: Feedstocks data**

	Dimension (mm)	Rubber wood
Ultimate data %	C	50.6
	H	6.5
	O	42
	N	0.2
Proximate data %	Volatiles	81.1
	Fixed Carbon	19.1
	Ash	0.7
	Moisture	18.5

## 2.2 Geometry Development

Figure 1 shows the schematic diagram of the In this research, single-stage downdraft gasifiers were performed to determine the effects of producer gas due to steam and air as their gasification agents. Input delivery of the gasifying agent was performed through four injection nozzles, arranged in a radial 90° pattern. Both of the reactors have an injection nozzle internal diameter of 0.07 m and an elevation of 1.75 m (from the top of the reactor to the ashtray). These gasifier models are designed by using Solidworks and the details of these gasifiers can be discovered in Table 2.

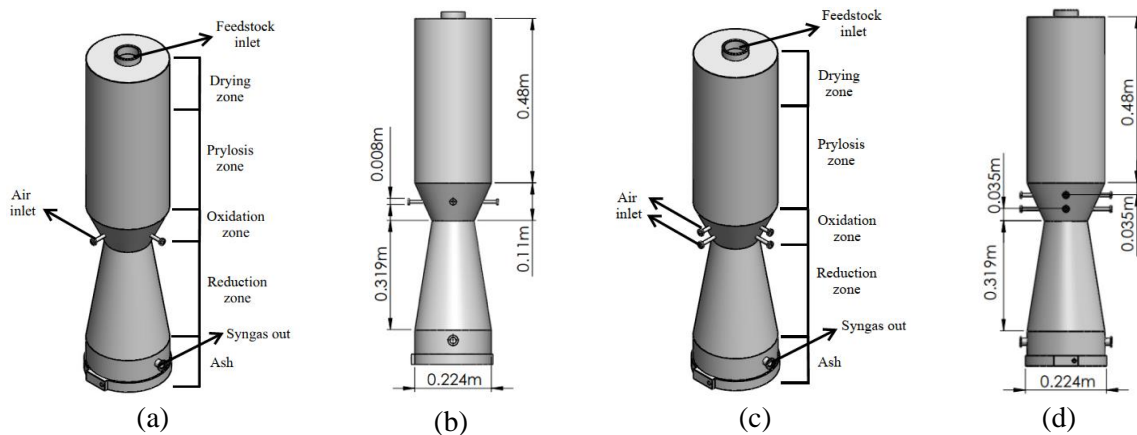


**Figure 1: Downdraft gasifier for (a) single stage (b) schematic view single stage (c) double stage (d) schematic view double stage**

**Table 2: Dimension of gasifier**

Part of Gasifier	Dimension (mm)
Height of gasifier	1.009
Throat diameter	0.122
Thickness of shell	0.010
Injection nozzle diameter	0.008
Feedstock inlet diameter	0.060
Syngas outlet diameter	0.020

Only for the double-stage downdraft gasifier, the first inlet is 0.035 m below pyrolysis zone and second inlet is 0.035 m above reduction zone. Figure 1 shows a schematic diagram of a downdraft gasifier with the various zones (drying, pyrolysis, oxidation/combustion, and reduction). For single-

stage downdraft gasifier, starting from the bottom, the base of the gasifier was designed with a diameter of 0.224 m. Above the base of the gasifier, one fuel outlet of 0.002 m diameter was placed at a height of 0.07 m. All reactions of the oxidation zone occur between 0.300 m and 0.590 m in the gasifier. As illustrated in the diagram, the air is directed into the combustion zone as a gasification agent through the four air nozzles. The diameter of each air nozzle is 0.00823 m. Then the throat of diameter and thickness of shell is 0.122 m and 0.010 m. At the same time, biomass is fed from the top of the gasifier with diameter 0.060 m. The gasifier stood at a total height of 1.009 m. Additional details about parameters of gasifier design can be found in Table 2.

### 2.3 CFD modelling analysis

The temperature gases. Gasification thermochemical processes of biomass are analysed using the robust (2D) and modelling method of CFD (Computational Fluid Dynamics). The model covers all four gasifier zones, namely drying, pyrolysis, oxidation and reduction. The composition of the various gas species resulting from the volatile break-up during gasification is being evaluated step-by-step. However, the selection of suitable CFD modelling chemical reactions is problematic, as the common reactions used in kinetic studies show discrepancies in the prediction of the compounds of the CFD synthesis gas. The use of computational tools to simulate real problems is of considerable value because design costs are reduced, allowing different geometries and fuels to be evaluated in gasifiers without necessarily constructing a reactor or having the energy. But the computational model must therefore be valid and compared with real experimental data. It can be seen as a mathematical model that makes future projects easier and faster if the final PCI values are closely compared. Ansys FLUENT® was therefore used under the limiting conditions for this study<sup>15</sup>. For this study, computer tools such as SolidWorks® are used to design the gasifier geometry and Ansys FLUENT® for thermochemical process simulation to achieve a gas synthesis of different types of biomass. Therefore, the study proposes a revised set of chemical mechanisms and the robustness of the approach is examined with validated results against literature data. The model will then be used to study biomass feedstock syngas production.

### 2.4 Governing Equations

At the start achieved. At the current time, Eulerian-Lagrangian and Eulerian-Eulerian approach mainly comprises the two types of methods for CFD bio-gasification simulations. In the Eulerian-Lagrangian method, the Navier-Stokes equations describe the gas phase, while the solid phase is considered a discreet one. In the meantime, the Eulerian-Eulerian solution requires less calculation as the reliable process is viewed as a continuum. Newtons Laws of Motion determine the trajectory of each particle, and the soft-sphere or hard-sphere model represents the particle collisions. For every particle, energy equations are determined by other variables, such as temperature and gas concentration. The equations governing the simulation study included mass conservation, conservation of moments, energy equation, transport equation and the model for the transport of species shown in Eq.1, Eq.2, Eq.3 and Eq.4.

#### 2.4.1 Momentum Conservation Equation

The momentum equation based on the Newton laws of motion is based on an acceleration rate that refers to the sum of forces that act on a flowing element which is the momentum change rate for the resulting force. Therefore, the equation for momentum conservation can be written as follows:

$$\frac{\partial(\rho\vec{v})}{\partial t} + \nabla \cdot (\rho\vec{v}\vec{v}) = -\nabla \cdot p + \nabla \cdot (\vec{\tau}) + \rho\vec{g} + \vec{F} \quad Eq.1$$

where  $p$  is the static pressure,  $\rho\vec{g}$  and  $\vec{F}$  are the gravitational body force and external body force respectively<sup>16</sup> Also,  $\vec{\tau}$  refers to stress tensor.

### 2.4.2 Mass Conservation Equation

The general form of the equation of mass conservation known as the equation of continuity is written:

$$\frac{\partial \rho}{\partial t} + \nabla \cdot (\rho \vec{v}) = S_m \quad Eq.2$$

where  $S_m$  is the mass added from the second phase in the continuous phase <sup>16</sup>.

### 2.4.3 Energy Conservation Equation

The conservation of energy is based on the first law of thermodynamics. The internal energy by system needs to equate with the heat absorption system without the system having to do its job. In general, the following may be written:

$$\frac{\partial}{\partial t} (\rho E) + \nabla \cdot (\vec{v}(\rho E + \rho)) = \nabla \cdot (k_{eff} \nabla T - \sum_{j=1}^N h_j \vec{J}_j + (\tau \cdot \vec{v})) + S_h \quad Eq.3$$

The effective thermal conductivity is  $k_{eff}$  ( $k + k_t$ , where  $k_t$  is the turbulent thermal conductivity). The first three terms on the right-hand side of the equation (3.3) represent a heat flow due to Fourier's conduction law, species diffusion, and viscous dissipation due respectively to normal shear stress <sup>16</sup>

### 2.4.4 Transport Equation for Standard K-Epsilon

Due to its robustness and reasonable accuracy for a wide variety of streams, the standard k- $\epsilon$  model is one of the most used turbulence models in computational fluid dynamics. The k- $\epsilon$  is a half-empirical model based on transport equations and its rate of dissipation rate for turbulent kinetic energy k. It is assumed that the model's derivation is totally turbulent and that the molecular viscosity effects are negligible. The transport equations and dissipation rate are defined as follows for turbulent cinematic energies:

$$\frac{\partial}{\partial t} (\rho k) + \frac{\partial}{\partial x_i} (\rho k u_i) = \frac{\partial}{\partial x_j} \left[ \left( \mu + \frac{\mu_t}{\sigma_k} \right) \frac{\partial k}{\partial x_j} \right] + G_k + G_b - \rho \epsilon - Y_m + S_k \quad Eq. 4$$

where  $S_k$  is the source terms for k and  $\epsilon$ , and  $G_k$  is the term for the turbulent kinetic energy production due to the mean velocity gradient<sup>16</sup>.

### 2.5 Turbulence Model

The CFD turbulence model was used to model the downdraft gasification process in the ANSYS-Fluent software related to the gasification process. The k- $\epsilon$  turbulence analysis is used to evaluate the viscosity of  $\mu_t$  turbulence using the kinetic energy of vortices and the dissipation rate (the loss of fluid energy over time due to friction or turbulence)<sup>17</sup>. The following equation expresses the turbulence viscosity model.

$$\mu_t = C_\mu \frac{k^2}{\epsilon} = \frac{\mu_t}{\rho} \quad Eq. 5$$

The forms of the transport equation for turbulent kinetic energy k and dissipation are as follows <sup>17</sup>:

- i. For kinetic energy of turbulence

$$\frac{\partial k}{\partial t} + \text{div}(k\vec{u}) = \text{div} \left( \frac{\mu_t}{\sigma} \text{grad}(k) \right) + p - \epsilon \quad Eq. 6$$

ii. For dissipation energy

$$\frac{\partial \varepsilon}{\partial t} + \text{div}(\varepsilon \bar{u}) = \text{div} \left( \frac{\mu_t}{\sigma_\varepsilon} \text{grad}(\varepsilon) \right) + C_{\varepsilon 1} \frac{p\varepsilon}{k} - C_{\varepsilon 2} \frac{\varepsilon^2}{k} \quad \text{Eq. 7}$$

Some previous literature has used the k-turbulence model for numerical simulation of the gasification process. In addition, the pressure-based solver was used to solve the flow equations and species using the second-order scheme as a spatial discretization scheme.

## 2.6 Multiphase Model

Biomass gasification is a multiphase flow process where a few phases exist simultaneously. Depending on the case situation and operating conditions, either the Eulerian-Lagrangian or the Eulerian-Eulerian method can be employed to simulate multiphase reactive flows inside<sup>18</sup>. The heterogeneous char reactions in the experimental test rig are modelled using a CFD model based on the software ANSYS Fluent 19.5. The numerical model follows the Eulerian-Eulerian technique, often known as the two-fluid model (TFM).

Interpenetrating continua are assumed to exist between the gas phase and the solid phase. Following the kinetic theory of granular flow, the continuity equation, Navier-Stokes equation, and energy equation for the granular phase are closed by defining granular pressure, granular viscosity, and granular stress as functions of granular flow (KTGF)<sup>19</sup>. The granular temperature is added as a new balance equation that allows for time-dependent and non-uniform distributed particle velocity fluctuations<sup>19</sup>.

The Eulerian multiphase model is multiphase flow models because of the significant coupling effect between the continuous and dispersed phases. Its solution is based on a single pressure shared by all phases, with each phase's continuity, momentum, and energy equations computed separately<sup>20</sup>. In the Eulerian model, several interphases drag coefficient functions are appropriate for different sorts of multiphase regimes. Typically, phase coupling through inter-phase exchange terms is characterized using drag coefficient models expressed in local Reynolds numbers<sup>20</sup>.

## 2.7 Grid Development

Meshing is used to fragment a structure into smaller parts to measure structure parameters with increased accuracy. During meshing, a limited number of grid points are generated in the structure known as nodes. The control equations are numerically solved at these nodes for the desired parameters. The governing equations resolved at the nodes in this model were described in Section 3.5. The finite volume method is used to solve these equations. The higher the density of the meshing, the greater the precision of problem-solving. But higher accuracy is at the expense of more complexity in solving equations. Therefore meshes must be generated in a balance with the adequate density to collect data but with a relatively low density, when equations can be resolved by software instantly<sup>21</sup>. Thus, the curvature capture is the element of the meshing process in this study. Meshing of model is shown in the Figure 2 with the details in the Table 3.

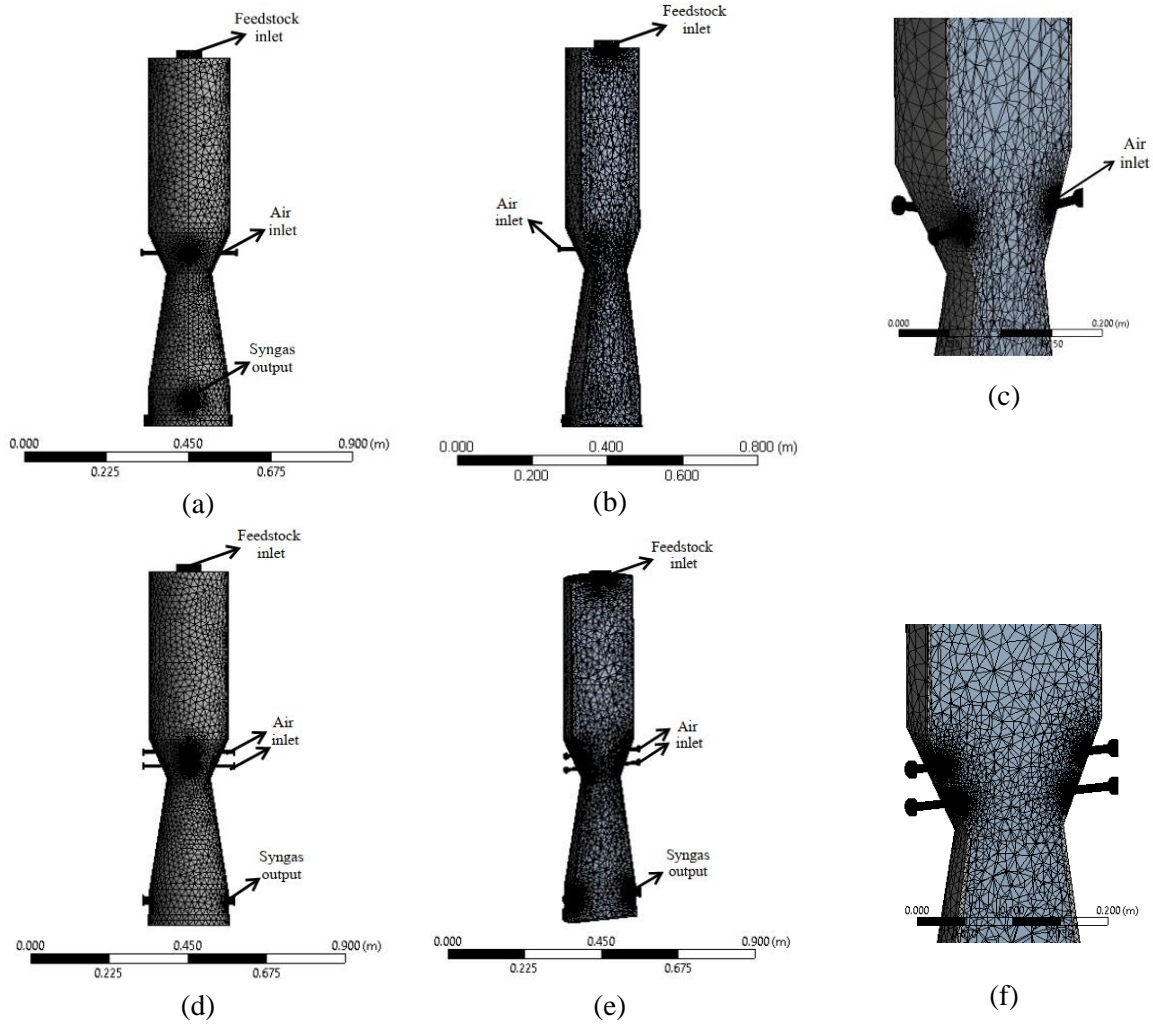


**Figure 2: Model in predominantly tetrahedron cell (a) single stage (b) side view single stage (c) cross section double stage (d) double stage (e) side view double stage (f) cross section double stage**

**Table 3: Meshing details**

<b>Properties</b>	<b>Single stage model</b>	<b>Double stage model</b>
Volume	2.9609e <sup>-002</sup> m <sup>3</sup>	2.9619e <sup>-002</sup> m <sup>3</sup>
Centroid X	1.5793e <sup>-006</sup> m	2.9603e <sup>-007</sup> m
Centroid Y	0.53951 m	0.53949 m
Centroid Z	3.8371e <sup>-007</sup> m	2.9265e <sup>-006</sup> m
<b>Statistics</b>	<b>Single stage model</b>	<b>Double stage model</b>
Nodes	65595	111241
Elements	333138	561374
Mesh Metric	Skewness	
Minimum	8.47720402931129e <sup>-05</sup>	8.26741124595465E-05
Maximum	0.797040365651879	0.799737517180896
Average	0.229225275016671	0.230278600227688
<b>Sizing</b>	<b>Single stage model</b>	<b>Double stage model</b>
Curvature Min Size	10.0°	10.0°
Bounding Box Diagonal	1.0946 m	1.0946 m
Average Surface Area	1.8531e <sup>-002</sup> m <sup>2</sup>	1.351e <sup>-002</sup> m <sup>2</sup>
Minimum Edge Length	1.e <sup>-003</sup> m	1.e <sup>-003</sup> m
<b>Quality</b>		

	Single stage model	Double stage model
Smoothing	High	
Minimum	8.4772e-005	8.2674e <sup>-005</sup>
Maximum	0.996	0.99852
Average	0.31001	0.31783
Standard Deviation	0.22909	0.2385
<b>Inflation</b>		
	Single stage model	Double stage model
Inflation Option	Smooth Transition	
Transition Ratio	0.272	

The problem domain is divided into a large number of tiny cells during mesh development. The number of cells in the domain has a significant impact on the simulation outcomes. Two models were done meshing by using ANSYS Fluent software. The volume for single stage model is 2.9609e-002 m<sup>3</sup> and double stage model 2.9619e-002 m<sup>3</sup>. Grid Independence study of the single stage downdraft gasifier was done by meshes 65595 while for double stage downdraft gasifier is 111241. Then the curvature minimum size for two models are 10.0° and bounding box diagonal for single stage model is 1.8531e-002 m<sup>2</sup> while for double stage model 1.0946 m. The quality meshing for both models are smoothing. Next, the average quality for the single stage downdraft gasifier is 0.31001 and for double stage downdraft gasifier 0.31783. Moreover, the inflation for both models are smooth transition and the transition ratio are 0.272.

## 2.8 Non-Premixed Combustion Model

A non-premixed model with the Probability-Density Function (PDF) the approach is selected to model the gasification process. It is developed explicitly for turbulent diffusion flames. The non-premixed model with the Probability-Density Function, assuming that the reaction chemistry is sufficiently rapid for equilibrium, this model can predict the production of intermediate species, dissociation effects, and rigorous turbulence-chemistry coupling using a chemical equilibrium approach<sup>22</sup>. These are achieved by pre-calculating the variables and then solving the transport equation. Then, saving the results in a look-up PDF table for use as a reference throughout the simulation process<sup>22</sup>.

## 2.9 Boundary Condition

For air injection into the combustion zone, four air nozzles are used, the amount of air illustrated in Table 4 at the model for every inlet. For single stage gasification, the air inlet is 0.05 m above grate. Then, the first inlet for double stage downdraft gasifier is 0.035 m above the grate, whereas the second inlet is 0.245 m below the first inlet. The main concept for injecting the gasifying agent from two different locations is to separate the pyrolysis zone from the reduction zone to obtain significant tar reductions. Biomass is fed from the top of the gasifier, while the total number of particles is tracked using a Lagrangian technique (Discrete phase). The discrete phase model uses an Euler-Lagrange approach. The Navier-Stokes equations solve the first phase, which represents the fluid. The second phase, which represents dispersed particles, is solved by monitoring a particular number of particles across the flow field. Within each phase, mass, momentum, and energy are exchanged. Finally, this gas stream (syngas) flows through the bottom of the reactor, where a mixture of unconverted carbon and ash.

**Table 4: Boundary conditions**

Part of Gasifier	Rubber wood
Equivalence ratio	0.326
$\dot{m}$ fuel, kg/s	0.0010138889
$\dot{m}$ air, kg/s	0.0016666667
Air T, K	600
Biomass T, K	300

## 2.10 Simulation Procedure

ANSYS Fluent 19.2 CFD software was used for numerical simulation in this analysis. ANSYS Fluent simulation setup consisted of geometry development, geometry import and mesh, CFD pre-production, CFD simulation solving, and CFD post-processing. After its construction in Solidworks 2018, the geometry of ANSYS Workbench has been designated as poly solids. The model was meshed with ANSYS Mesh forms of a tetrahedron and set the gravity of the y-axis at  $9.81 \text{ ms}^{-2}$ . The setup program was introduced. Fluent has defined the solver preferences. A K- $\epsilon$  turbulence model has been developed with possible near-wall treatment. Therefore, in this simulation analysis, the achievable k- $\epsilon$  model was used to capture the gas phase turbulence flow inside the gasifier with the standard wall functions. For species transportation and volumetric reaction, the non-premixed combustion was described. In addition, the state relation have been determined with the chemical equilibrium. By the proximate and ultimate analysis, the reaction fuel is described. Fuel injection uses a discrete phase with a uniform type of combustion particles. Then, it defines all the boundary conditions and the set of parameters listed to solve the pressure-velocity coupling, the SIMPLE algorithm scheme was used and the standard scheme was chosen for the pressure discretization. After grid independence studies were completed, the second-order upwind scheme was introduced to obtain precise results for other measured variables. Finally, using standard initialization, the simulation configuration was initialized and the calculation was run with an iteration number of 3000.

## 3. Results and Discussion

In this section, CFD analysis studies using the ANSYS Fluent software are presented for the composition of syngas yield and temperature distribution along the gasifier. This simulation work applied to both design of the model gasifier which are single-stage and two-stage downdraft reactor. A comparative result between the single-stage and two-stage gasifier is introduced to study the performance of the reactor.

### 3.1 Model Validation

Figure 3 shows the gas composition for the three data sets at the gasifier outlet. A detailed analysis of Figure 3 shows that the results of  $\text{H}_2$  content for the present model was lower than the results reported by Kumar & Paul (CFD/Experiment) and Salem et. al. (Experiment). The deviation occur as the CFD model is entirely non-equilibrium. A typical model for gasification which using air as an oxidation agent is typically convenience in determining the concentration of CO and  $\text{H}_2$  species if the relative error is around 10.00 %<sup>23 24</sup>. This work demonstrated significant agreement in this regard, as the relative error for the two species ranges from 2.5 to 5.2%. In all cases when  $\text{CH}_4$  is produced utilising air as a gasification fluid, the relative inaccuracy reported in the literature consistently displays a higher discrepancy<sup>23 24 25</sup>. This present results shows that the CFD model simulated values of outlet gas composition was in good agreement with the Paul<sup>1</sup> model prediction and experimental data<sup>2</sup>. Thus, it is considered that the present simulation model was applicable to be used for the analysis in this study.

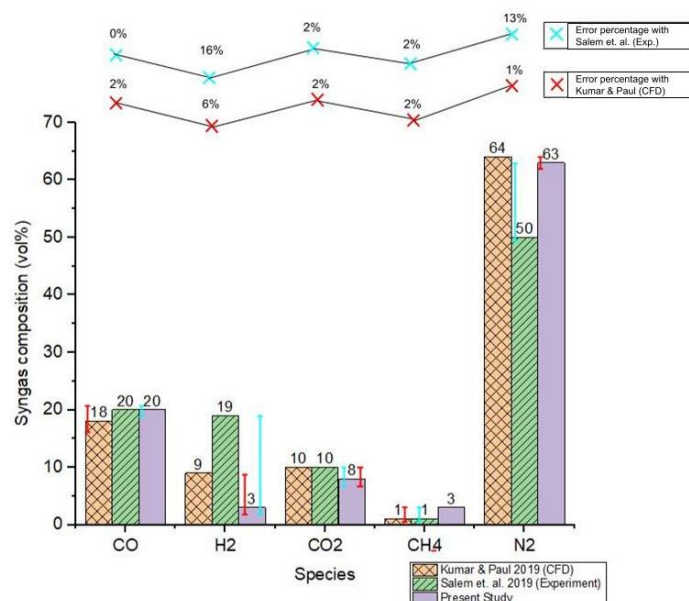


**Figure 3: Comparison of synthesis gas composition against species**

### 3.2 Temperature Distribution in Gasifier

Figure 4 (a) illustrates the performance of the gasifier based on temperature contour from different zones. The data clearly show that the oxidation zone, located near the gasifier's centerline and has a temperature of 602K for single stage while 603K for double stage gasification, is higher than the reduction and pyrolysis zones. The peak temperature, or ignition temperature, (602–603) K, can be seen near the air injection points; however, this is not the combustion temperature. The temperature drops to normal levels in the middle of the gasifier. This behaviour was described in <sup>2</sup>.

The reactor temperature is one of the important operational parameter for gasification because the main gasification reactions are endothermic. Figure 4 (b) depicts the CFD model predicted reactor temperature contours and a direct relationship between gasifier height and temperature in the various zones for single and double stage gasification. The highest temperature inside the gasifier for a single stage model is found in the oxidation zone, where the air is supplied. The temperature in the drying zone is less than 460 K, in the pyrolysis zone is between 470 and 455 K, in the oxidation zone is between 470 and 490 K, and in the reduction zone is between 480 and 485 K.

Oxidation zone reaction play an important role for gasification of biomass in downdraft gasifier. Because all the species release from the volatile and char comes first time, get contact with the air in the oxidation zone. All the oxidation zone reactions taking place in the gasifier at height between 0.3 m and 0.59 m. All the reduction zone reactions taking place in the reduction zone (0–0.26 m). Further, the reduction zone reactions also occur in the oxidation zone because the temperature in that zone is high and consequently, the endothermic reactions are trigger in this zone, height from 0.34 m to 0.46 m.

The highest temperature inside the gasifier for a double stage model is found in the oxidation zone, where the air is supplied. The temperature in the drying zone is less than 470 K, in the pyrolysis zone is between 470 and 480 K, in the oxidation zone is between 470 and 520 K, and in the reduction zone is between 480 and 485 K. Gasification process with two stages of air supply highlighting the importance of the pyrolysis zone for the tar conversion efficiency: the stabilization of this zone is dependent of the balance between downward solid movement and upward flame propagation. If the rubber wood particles move faster (downward) than the flame propagation (upward), the oxidation zone reaches the second air intake thus enabling the whole system to act like a single-stage gasifier. If flame propagation upward exceeds the biomass consumption, both stages remain in stable operation (EconPapers: Multi-Stage Reactor for Thermal Gasification of Wood, n.d.). The CO, CH<sub>4</sub> and H<sub>2</sub>

concentrations of this work agree with those reported by Andrade <sup>11</sup>. The author <sup>11</sup>, in experiments on wood gasification in a downdraft gasifier showed the advantages of the double stage air supply configuration: tar concentration in the producer gas was reduced more than thirteen times.

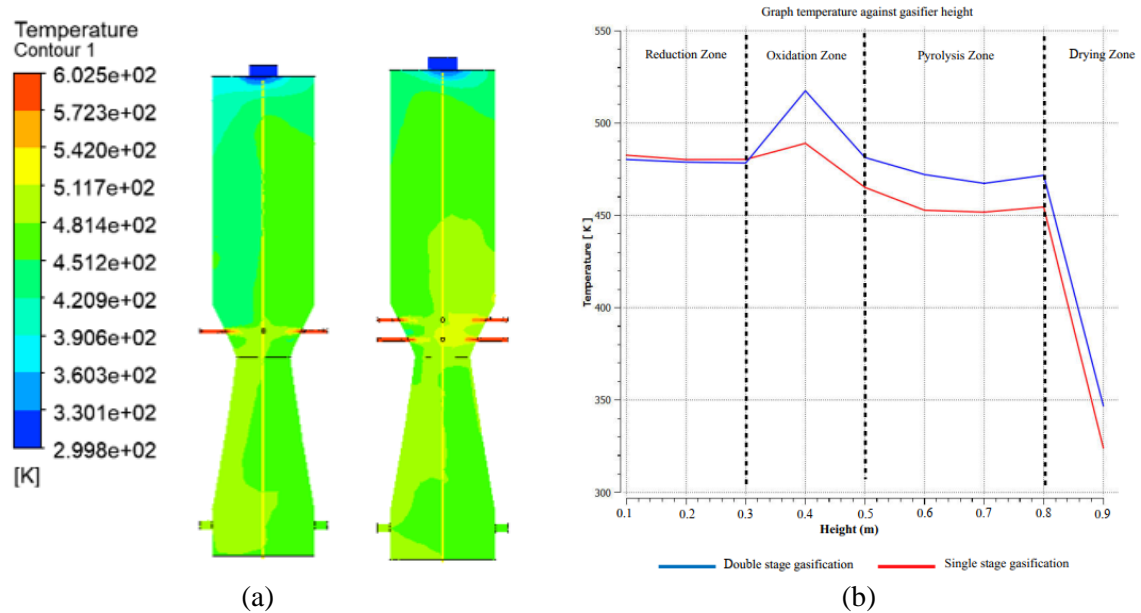


**Figure 4: (a) Comparison of temperature for single and double stage (b) plot of the relationship between temperature against gasifier height**

### 3.3 Species distribution (contours)

Figure 5.(a) (b) (c) (d) and (e) shows the distributions of species formation between single stage and double stage gasification, including gases formation. When biomass fuel enters the gasifier, it undergoes a volatile process that produces mainly CO, CO<sub>2</sub>, CH<sub>4</sub>, H<sub>2</sub>, and N<sub>2</sub>. The synthesis gas is formed when char combines with gas species such as O<sub>2</sub>, H<sub>2</sub>, and CO<sub>2</sub>. The main reactions involving O<sub>2</sub> component was typically occurred in the oxidation zone, whereas other reactions seem to occurred in the reduction zone. It is observe that the CO and H<sub>2</sub> concentrations are higher in the pyrolysis zone as the volatile matter turn to gases phase due devolatilization process. The pyrolysis zone is where the devolatilization takes place. When the released gases CO and H<sub>2</sub> reach the oxidation zone, they react with oxygen and convert to CO<sub>2</sub> and H<sub>2</sub>O, respectively. However, due to the limited availability of oxygen, not all CO and H<sub>2</sub> are transformed into CO<sub>2</sub> and H<sub>2</sub>O. However, in the reduction zone, CO<sub>2</sub> and H<sub>2</sub>O react with char to form CO and H<sub>2</sub> <sup>2</sup>. The contour plots also show that the hydrogen and carbon monoxide compositions are higher than the other gas compositions. Water gas shift and methane steam reforming processes are the primary sources of hydrogen.

As shown in Figure 5 (a) and (b), CO and H<sub>2</sub> have the same trend along the gasifier. During the gasification of rubber wood, the findings were obtained. The devolatilization process promote the production of CO and H<sub>2</sub> and gradually increased and slightly above the combustion zone due to gas reactions in pyrolysis. H<sub>2</sub> and CO are consumed and transformed to other gases (CO<sub>2</sub>, H<sub>2</sub>, and tar) during combustion. After combustion, the species at reduction zone begins to slightly increase in their value due to gasification reactions and air reactions. Because both processes have a slow reaction rate, the synthesis of CO and H<sub>2</sub> is decreased.

Figure 5 (d) shows that the distribution of CH<sub>4</sub> was apparently identical with CO and H<sub>2</sub> species. It is formed during pyrolysis and reaches its maximum value at the end of the process and then decrease in its amount during combustion. The amount of methane released during pyrolysis is still minimal due

to the methane oxidation reaction. Furthermore, it begins to form again in the reduction zone due to methanation processes. As seen in Figure 5 (c), CO<sub>2</sub> indicates a different trend than CO, CH<sub>4</sub>, and H<sub>2</sub>. It begins release with volatiles in the pyrolysis zone and consistently increase in the oxidation zone due to oxidation processes until it reaches its maximal value. Then, due to gasification, it decreases slightly again during reduction.

The N<sub>2</sub> formation contours inside the gasifier are illustrated in Figure 5 (e). On the other hand, Air gasification produces significantly higher nitrogen (63.00 %). As shown in Figure 5, N<sub>2</sub> forms in the oxidation zone due to air injection. Oxidation has the highest nitrogen value, with greater volume concentrations at air injection, decreasing as other gases form in the reduction zone until exit points. This phenomenon was described in experimental data <sup>2</sup>, and others reported <sup>1</sup>.

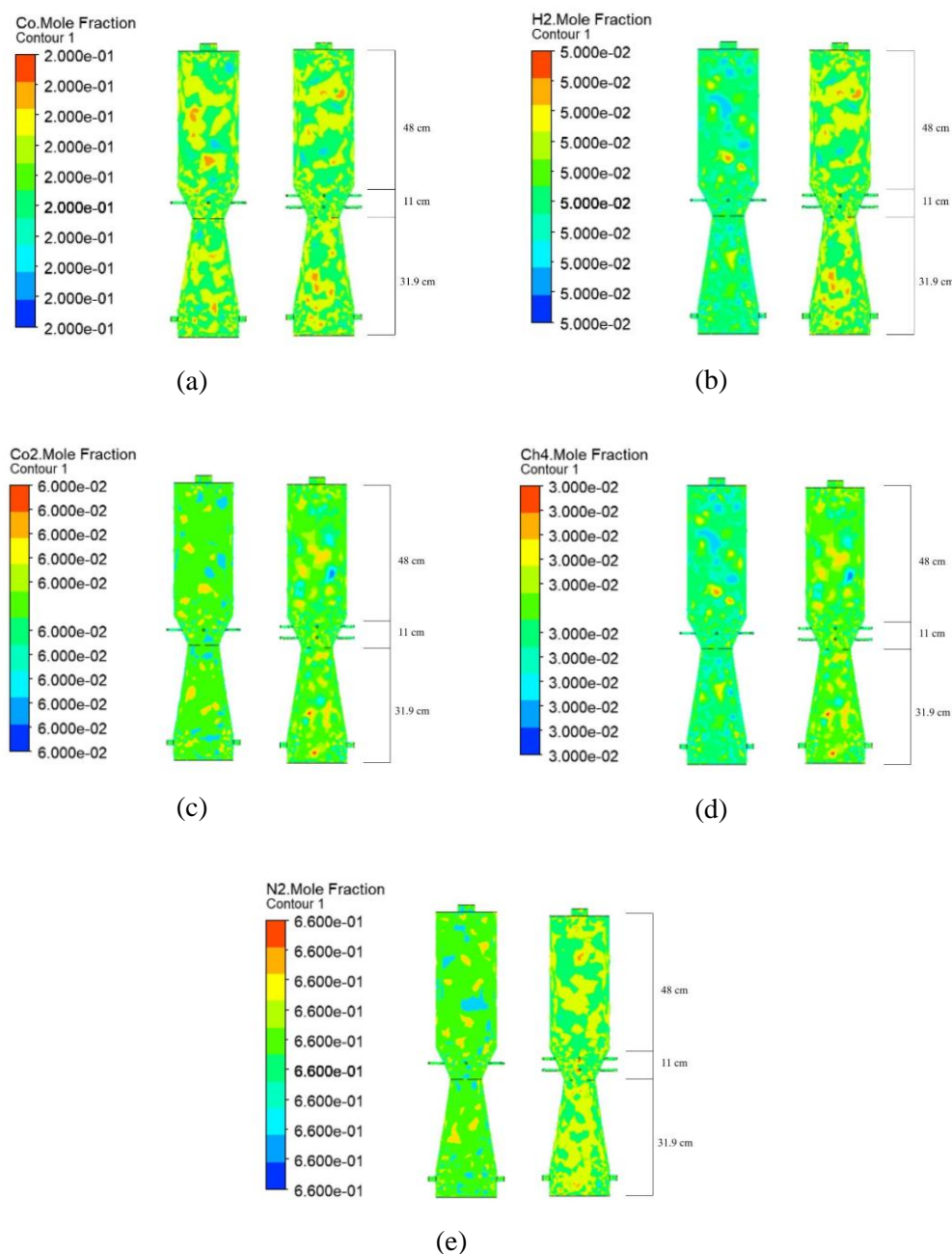


**Figure 4: Comparison of mole fraction for single stage and double stage**  
 (a) CO (b) H<sub>2</sub> (c) CO<sub>2</sub> (d) CH<sub>4</sub> (e) N<sub>2</sub>

### 3.4 Graph species distribution

According to Figure 6, air is used as a gasification agent in single stage and double stage to produce CO concentrations in the combustion zone. The value of CO mole fraction for single stage and double stage exactly same 0.20 % in CFD model. These results are in agreement with the <sup>26</sup>. Based on the distribution of CO species as in Figure 4, the location with the largest concentration of this species, according to the results of the CFD model, is located at the interface between the combustion and gasification zones. The concentration increases as it gets closer to the reactor core. The process characteristic was also described in the experimental data reported by<sup>2</sup> and <sup>1</sup>.

In addition, the concentration of H<sub>2</sub> mole fraction was 0.03 % and 0.05 % for single and double stage respectively. Figure 6 shows the concentration of H<sub>2</sub> mole fraction for single and double stage during gasification at different stages. Higher temperatures favour gasification fluids in exothermic reactions and products in endothermic reactions, consistent with the experimental results. This result was described in experimental data <sup>2</sup> from this study and others recently published<sup>1</sup>.

Then, Figure 6 presents the comparison of CO<sub>2</sub> mole fraction where the single stage was 0.08% while the double stage was 0.06 %. The mole fraction of CO<sub>2</sub> increased since the mole fraction of N<sub>2</sub> increased. Meanwhile, the rate of reactions in the reduction zone and the length of the reduction zone influence CO<sub>2</sub> production.

Furthermore, according to Figure 6 the comparison of CH<sub>4</sub> mole fraction against model. where the single stage was 0.06 % while the double stage was 0.03 %.<sup>27</sup> reported CH<sub>4</sub> values similar to those found in this study. It is demonstrated the advantages of the double stage by supply air in gasification experiments in a downdraft gasifier. Although the CH<sub>4</sub> concentration in downdraft gasifiers is minimal, it contributes significantly to the syngas heating value. According to earlier research <sup>28</sup> <sup>29</sup>, carbon gasification with air, which occurs shortly after biomass drying and devolatilization, promotes CH<sub>4</sub> production. The CH<sub>4</sub> concentration profiles generated from the CFD simulation are shown in Figure 4. Because air reforming or thermal cracking of CH<sub>4</sub> is not encouraged, low quantities of CH<sub>4</sub> were reported at lower temperatures. This explains why the gasification zone has lower concentrations, and the drying zone has essentially no visible contour. These findings are in line with the results obtained in this study. Several researchers who researched into two-stage reactors came up with similar findings <sup>30</sup>.

Finally, Figure 6 shows the trends of N<sub>2</sub> mole fraction for single stage and double stage model. The value for single stage was 0.63 % while double stage was 0.66 %. Because of the volatile release gases after devolatilization, CO and H<sub>2</sub> concentrations are higher in the pyrolysis zone. The pyrolysis zone is where the devolatilization takes place. When the release gases CO and H<sub>2</sub> reach the oxidation zone, they react with oxygen and convert to CO<sub>2</sub> and H<sub>2</sub>O, respectively. The air to biomass ratio represents the amount of oxygen injected into the gasifier and influences the gasification temperature. The higher the air to biomass ratio, the higher the gasification temperature, which accelerates the gasification process due to increased oxygen content and, as a result, improves the purity of the product to some extent. In addition, the findings revealed that as the air to biomass conversion rate increases produce more heat is emitted cause increasing H<sub>2</sub>. The temperature increase in the pyrolysis and combustion zones implies that the two air supplies affect the tar and particle content in the producing gas. The temperature in the pyrolysis zone is significantly higher, increasing the combustion zone temperature. This behaviour was described by <sup>11</sup>.

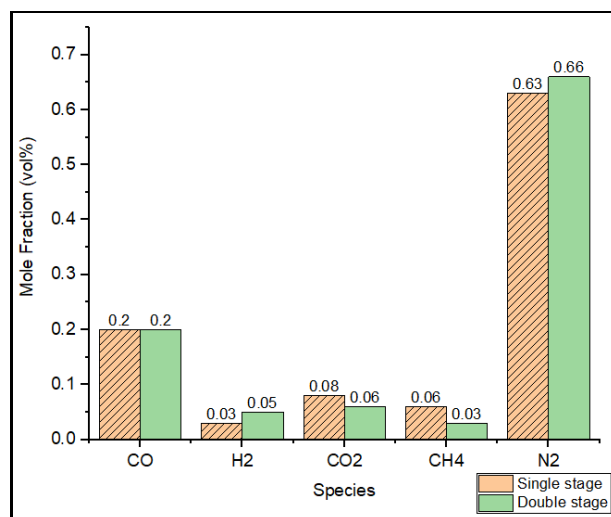


Figure 5: Comparison of mole fraction against species

#### 4. Conclusion

ANSYS software was used to create the 2D CFD model. The model was capable of simulating the operation of air-blown downdraft gasifiers. The model was initially tested against single and double stage gasification and found to be in good agreement. The model was also used to investigate the gasification process with rubber wood as a feedstock. In addition, the model was used to investigate syngas composition and temperature along gasifiers. The results of the syngas species formation were validated against previous research <sup>1</sup> and experimental data carried out by other researchers <sup>2</sup>.

The model is a four-zone kinetic model with the outcomes of each zone feeding into the next. A novel feature was used in developing the model based on the total char consumption at the reduction zone. Based on this assumption, the length of the reduction zone was calculated, as were all syngas products. The model was also able to successfully design downdraft gasifiers based on gasifier capacity and feedstock. Furthermore, key design parameters such as throat diameter and gasifying agents are discussed to optimize the design process and produce a gasifier capable of accommodating fuel changes and other working conditions for higher syngas production. The highest syngas composition was N<sub>2</sub> 0.63 (vol %), while the lowest syngas composition was H<sub>2</sub> 0.03. (vol %). The trend for result syngas composition is the same for single and double stage gasification.

Furthermore, the influence of changing working parameters on the distribution of different gas species along the gasifier was discussed. The temperature variation within the gasifier, as well as the gasification temperature, were investigated. According to the results obtained under the tested conditions, airflow is an important characteristic in the operation of downdraft gasifiers. The findings imply that secondary stage air supply has a significant impact on reducing CH<sub>4</sub> concentrations in the product gas, linked to tar reductions. These conditions suggest that biomass devolatilization in the pyrolysis zone produces lighter compounds that are easier to fracture when the gas stream passes through the combustion zone. This phenomenon is the cause of the low CH<sub>4</sub> content in this situation.

In summary, several key conclusions can be taken away from this analysis:

- Rubberwood gasification technology providers have a great opportunity in large, high-growth mega-markets of energy.
- Gasification is a clean energy technology.
- Rubberwood will be utilized heavily to fuel much of the global growth.
- Gasification is the best option for rubberwood in a CO<sub>2</sub>-constrained world.

## Acknowledgement

The authors would like to thank the Faculty of Engineering Technology, Universiti Tun Hussein Onn Malaysia for its supports.

## References

- [1] Kumar U, Paul MC. CFD modelling of biomass gasification with a volatile break-up approach. *Chem Eng Sci.* 2019;195:413-422. doi:10.1016/j.ces.2018.09.038
- [2] Salem AM, Zaini IN, Paul MC, Yang W. The evolution and formation of tar species in a downdraft gasifier: Numerical modelling and experimental validation. *Biomass and Bioenergy.* 2019;130:105377. doi:10.1016/j.biombioe.2019.105377
- [3] Galindo AL, Lora ES, Andrade RV, Giraldo SY, Jaén RL, Cobas VM. Biomass gasification in a downdraft gasifier with a two-stage air supply: Effect of operating conditions on gas quality. *Biomass and Bioenergy.* 2014;61:236-244. doi:10.1016/J.BIOMBIOE.2013.12.017
- [4] Vaka M, Walvekar R, Rasheed AK, Khalid M. A review on Malaysia's solar energy pathway towards carbon-neutral Malaysia beyond Covid' 19 pandemic. *J Clean Prod.* 2020;273:122834. doi:10.1016/j.jclepro.2020.122834
- [5] WEO-2013 Special Report: Southeast Asia Energy Outlook – Analysis - IEA. Accessed June 20, 2021. <https://www.iea.org/reports/southeast-asia-energy-outlook-2013>
- [6] Azam M, Khan AQ, Zaman K, Ahmad M. Factors determining energy consumption: Evidence from Indonesia, Malaysia and Thailand. *Renew Sustain Energy Rev.* 2015;42:1123-1131. doi:10.1016/j.rser.2014.10.061
- [7] Cherp A, Vinichenko V, Jewell J, Brutschin E, Sovacool B. Integrating techno-economic, socio-technical and political perspectives on national energy transitions: A meta-theoretical framework. *Energy Res Soc Sci.* 2018;37:175-190. doi:10.1016/j.erss.2017.09.015
- [8] Flores JH, Peixoto DPB, Appel LG, De Avillez RR, Silva MIP Da. The influence of different methanol synthesis catalysts on direct synthesis of DME from syngas. In: *Catalysis Today.* Vol 172. Elsevier; 2011:218-225. doi:10.1016/j.cattod.2011.02.063
- [9] Segurado R, Pereira S, Correia D, Costa M. Techno-economic analysis of a trigeneration system based on biomass gasification. *Renew Sustain Energy Rev.* 2019;103:501-514. doi:10.1016/j.rser.2019.01.008
- [10] Sezer S, Özveren U. Investigation of syngas exergy value and hydrogen concentration in syngas from biomass gasification in a bubbling fluidized bed gasifier by using machine learning. *Int J Hydrogen Energy.* 2021;46(39):20377-20396. doi:10.1016/j.ijhydene.2021.03.184
- [11] Galindo AL, Lora ES, Andrade RV, Giraldo SY, Jaén RL, Cobas VM. Biomass gasification in a downdraft gasifier with a two-stage air supply: Effect of operating conditions on gas quality. *Biomass and Bioenergy.* 2014;61:236-244. doi:10.1016/j.biombioe.2013.12.017
- [12] in H, Fan C, Wei W, Zhang D, Sun J, Cao C. Evolution of pore structure and produced gases of Zhundong coal particle during gasification in supercritical water. *J Supercrit Fluids.* 2018;136:102-109. doi:10.1016/j.supflu.2018.02.016
- [13] Yepes Maya DM, Silva Lora EE, Andrade RV, Ratner A, Martínez Angel JD. Biomass gasification using mixtures of air, saturated steam, and oxygen in a two-stage downdraft

- gasifier. Assessment using a CFD modeling approach. *Renew Energy*. 2021;177:1014-1030. doi:10.1016/J.RENENE.2021.06.051
- [14] Biomass Gasification, Pyrolysis and Torrefaction: Practical Design and Theory - Prabir Basu - Google Buku. Accessed June 21, 2021. [https://books.google.com.my/books?hl=id&lr=&id=BYM2DwAAQBAJ&oi=fnd&pg=PP1&ots=nIny99sHtS&sig=LXCb9v1HIC5eDrWYziRx7NNNbpE&redir\\_esc=y#v=onepage&q&f=false](https://books.google.com.my/books?hl=id&lr=&id=BYM2DwAAQBAJ&oi=fnd&pg=PP1&ots=nIny99sHtS&sig=LXCb9v1HIC5eDrWYziRx7NNNbpE&redir_esc=y#v=onepage&q&f=false)
- [15] Frigo L, Santos DJ, Salgado M, Yepes Maya DM. Gasification of Alternative Biomass To Generate Power With Support of Cfd and Cad. 2019;(January). doi:10.26678/abcm.cobem2019.cob2019-1557
- [16] Prasertcharoensuk P, Hernandez DA, Bull SJ, Phan AN. Optimisation of a throat downdraft gasifier for hydrogen production. *Biomass and Bioenergy*. 2018;116:216-226. doi:10.1016/j.biombioe.2018.06.019
- [17] Janoszek T, Masny W. CFD Simulations of Allothermal Steam Gasification Process for Hydrogen Production. *Energies*. 2021;14(6):1532. doi:10.3390/en14061532
- [18] Chishty MA, Umeki K, Risberg M, Wingren A, Gebart R. Numerical simulation of a biomass cyclone gasifier: Effects of operating conditions on gasifier performance. *Fuel Process Technol*. 2021;218:106861. doi:10.1016/j.fuproc.2021.106861
- [19] Rößger P, Richter A. Numerical modeling of a batch fluidized-bed gasifier: Interaction of chemical reaction, particle morphology development and hydrodynamics. *Powder Technol*. 2021;384:148-159. doi:10.1016/j.powtec.2021.01.072
- [20] Lee SY, Sankaran R, Chew KW, et al. Waste to bioenergy: a review on the recent conversion technologies. *BMC Energy*. 2019;1(1):1-22. doi:10.1186/s42500-019-0004-7
- [21] Enget C, Jaojaruek K. CFD modeling of a downdraft gasifier with woodchips used as feedstock. *Int Energy J*. 2020;20(1):39-56.
- [22] Ren Z, Wang B, Zhao D, Zheng L. Flame propagation involved in vortices of supersonic mixing layers laden with droplets: Effects of ambient pressure and spray equivalence ratio. *Phys Fluids*. 2018;30(10):106107. doi:10.1063/1.5049840
- [23] Monteiro E, Ismail TM, Ramos A, Abd El-Salam M, Brito PSD, Rouboa A. Assessment of the miscanthus gasification in a semi-industrial gasifier using a CFD model. *Appl Therm Eng*. 2017;123:448-457. doi:10.1016/J.APPLTHERMALENG.2017.05.128
- [24] Cai J, Wang S, Kuang C. Experimental and Numerical Investigations on Gasification of Biomass Briquette in a Sectional Heating Gasifier. *Energy Procedia*. 2017;105:1234-1241. doi:10.1016/J.EGYPRO.2017.03.428
- [25] Murugan PC, Joseph Sekhar S. Species – Transport CFD model for the gasification of rice husk (*Oryza Sativa*) using downdraft gasifier. *Comput Electron Agric*. 2017;139:33-40. doi:10.1016/J.COMPAG.2017.05.004
- [26] Singh Siwal S, Zhang Q, Sun C, Thakur S, Kumar Gupta V, Kumar Thakur V. Energy production from steam gasification processes and parameters that contemplate in biomass gasifier – A review. *Bioresour Technol*. 2020;297:122481. doi:10.1016/j.biortech.2019.122481

- [27] Martínez JD, Silva Lora EE, Andrade RV, Jaén RL. Experimental study on biomass gasification in a double air stage downdraft reactor. *Biomass and Bioenergy*. 2011;35(8):3465-3480. doi:10.1016/j.biombioe.2011.04.049
- [28] Sharma T, Maya DMY, Nascimento FRM, et al. An Experimental and Theoretical Study of the Gasification of Miscanthus Briquettes in a Double-Stage Downdraft Gasifier: Syngas, Tar, and Biochar Characterization. *Energies* 2018, Vol 11, Page 3225. 2018;11(11):3225. doi:10.3390/EN11113225
- [29] de Sales CAVB, Maya DMY, Lora EES, et al. Experimental study on biomass (eucalyptus spp.) gasification in a two-stage downdraft reactor by using mixtures of air, saturated steam and oxygen as gasifying agents. *Energy Convers Manag*. 2017;145:314-323. doi:10.1016/j.enconman.2017.04.101
- [30] Yepes Maya DM, Lora ES, Andrade RV, Ratner A, Martínez JD. Biomass gasification using mixtures of air, saturated steam, and oxygen in a two-stage downdraft gasifier. Assessment using a CFD modeling approach. *Renew Energy*. Published online June 11, 2021. doi:10.1016/j.renene.2021.06.051